Experimental Results and Predictive Calculations for Pinhole Collimators Used in Small Animal Nuclear Imaging

Luke Ng

Senior Thesis

May 1, 2001

Abstract

Gamma-ray detectors for small animal imaging have generally used parallel hole collimators since they provide a good tradeoff between sensitivity to photons and image resolution. Pinhole collimators, on the other hand, can offer magnification of images from gamma-ray detectors, but at a cost of greater sensitivity to the positioning of the object being imaged and some distortion of the image. Current research has focused on determining the feasibility of using pinhole collimators to provide increased magnification. Understanding the tradeoffs involved in using pinhole collimators compared with parallel hole collimators has been an important aspect of this work. Phantoms loaded with ^{125}I and pinholes of various sizes have been designed and built for imaging runs, which test the sensitivity and the magnification of pinhole collimators.

Table of Contents

Introduction……..…Page 4

Mathematics of Pinhole Collimators …….....…….…….Page 9

Sources of Error ……..……..…...Page 11

Computational Work ……Page 12

Experimental Results ……...Page 14

Discussion and Conclusion ……..Page 21

Future Research ……Page 22

Appendix ……..Page 24

References ……Page 26

Introduction

Small animal imaging has interested scientists for several reasons. It gives an opportunity to image biological processes in small animals at the molecular level. Radioactive markers attached to biological ligands are injected into small animals. The detector uses parallel-hole collimators and segmented pixelated scintillators on position-sensitive photomultiplier tubes (PSPMT) to resolve images of the tagged ligands. These tubes record the planar location at which the photon made contact with the detector in two dimensions. These methods can similarly be applied in the imaging of breast cancer and brain tumors. There is the potential of providing previously unavailable information with detectors of better resolution than existing clinical nuclear medicine imaging detectors [1]. Current gamma-ray detector systems often use parallel-hole collimators, which provide reasonable imaging capabilities but no magnification. However, pinhole collimators are much more sensitive to the location of the object being imaged since a pinhole collimator can pick up photons that are traveling at an angle with respect to the axis parallel to the pinhole.

Audioradiography, Positron Emission Tomography (PET), and Magnetic Resonance Imaging (MRI), are alternative methods of imaging for biomedical applications. A brief overview of these techniques and their strengths and weaknesses will be provided in order to understand the main benefits of gamma-ray imaging.

Audioradiography consists of injecting the animal with a radioligand, waiting for it to circulate in the animal, sacrificing the animal, and slicing the tissue into very small pieces. These pieces are placed near a film containing silver bromide, where silver atoms are created when energy transferred from the radioligand separates the bromide from the

silver. The silver atoms show up as dark regions in the photographic film. This method has the advantage of producing high-resolution images since photographic film can display excellent detail. The main disadvantages are that it is only possible to take an image of a tissue sample after the animal has been sacrificed. A single tissue sample only gives a snapshot of the uptake of the radioligand, which forces one to use many samples in order to limit experimental errors. In addition, there is only a finite amount of silver bromide in the film. When all of it has reacted with photons, additional photons will not register on the film.

Positron Emission Tomography (PET) is a second method that has been used in biomedical studies. This method consists of using a ligand linked with a positron emitting isotope. The decay of the isotope causes the emission of a positron, which at rest will annihilate with an electron and cause the emission of two identical photons that are 180 degrees apart. These photons have an energy of 511 keV. Scintillators are placed around the animal to detect the specific location of the emitted photons and only accept photons that have a 180 degree separation. The main problem with PET is that the isotopes need to be produced with a particle accelerator, and these isotopes have very short half-lives. ^{11}C has a half-life of only 20 minutes while ^{15}O has a half life of only 2 minutes [2]. This presents great difficulties since most laboratories do not have cyclotrons capable of producing such short-lived isotopes.

Magnetic Resonance Imaging is a technique that uses a strong magnetic field to align the magnetic moments of the nuclei of the specimen with the field. Radiofrequency pulses are applied on the specimen, which causes the spins to flip. This allows the measurement of the time it takes for the magnetic moments to realign with the magnetic

field. This imaging technique is especially effective at picking out protons, which makes it useful in biological samples that are extremely aqueous. The main difficulty comes from imaging specimens that do not contain protons or have atomic nuclei, which have no spin. It is difficult to detect the magnetic signals of such nuclei.

Gamma-ray imaging provides several advantages over alternative imaging methods. The half-lives of the radionuclides (14 hours for ^{131}I to 60.3 days for ^{125}I) used in gamma-ray imaging allows one to take images over a longer period. This reduces the number of samples that need to be taken since it is possible to have one long image run instead of having many shorter runs.

In his dissertation, Dr. Andrew Weisenberger designed and described the use of gamma-ray imaging detector employed in this project [3]. The 125 mm diameter photon detectors consists of two gamma-ray cameras mounted on a gantry with a platform to hold a mouse. The gamma-ray camera system includes a computer connected to one or more position-sensitive photomultiplier tubes via a series of electronic circuits. Each photomultiplier tube is attached to view a CsI(Na) crystal scintillator consisting of small (1x1x3 mm) segmented pixels. A parallel hole CuBe collimator is attached to one of the scintillator. The camera can detect gamma rays released from the decay of ^{125}I, which penetrate the collimator and register on the scintillator and photomultiplier tubes. One of the main benefits of this detector is that it allows the observation of the metabolism of important molecules in small animals without the need to sacrifice the animals in order to determine the location of the injected radionuclide.

The apparatus was modified to include two 125 mm diameter detectors with one above and one detector placed below the platform. One of the detectors contains a

parallel hole collimator while the other detector utilizes a pinhole collimator. This setup allows an easy the comparison of the effectiveness of the two types of collimators.

This collaboration which includes Professors Saha and Bradley of the Biology department plus W&M and JLab physicists has used this detector to study the effects of certain drugs on mice. For example, mice have been anesthetized and a cocaine analogue injected into the mice with ^{125}I as the radioactive marker. The detector systems then which shows how the material is transported within the mouse.

In a number of previous experiments with pinhole collimators, ^{131}I has been used as the radioactive marker. Radiomarkers like ^{123}I, ^{67}Ga, ^{111}Im, and ^{99}Tc have also been used. There are several reasons why this project has used ^{125}I. The emitted photon from ^{131}I has about 364 keV, which would make scattering a more serious problem. Researchers use tungsten or other materials with a high Z as collimators to absorb the higher energy photons. Since ^{125}I emits much lower energy photons than ^{131}I, our pinhole collimators were made from brass, which is sufficient to limit scattering around the pinhole. As mentioned earlier, ^{125}I has a half-life of 60.3 days, and it emits a gamma ray photon of energy 35.3 keV and X-ray photons in the 27-32 keV range. This half-life is longer than that of most other potential markers, which allows the detect
or to record the binding of molecules on the brain and pancreas of the mice over a period of many hours or even days after the injection.

Converging and diverging collimators create distortion by expanding or contracting the image of the photons after they go through the collimators. They usually have lower sensitivity than parallel hole collimators, especially with thick objects [4]. Parallel hole collimators maintain the direction of the photon path and can offer greater

sensitivity than pinhole collimators. Pinhole collimators offer higher magnification when the object is closest to pinhole (see Fig. 1). This enhanced magnification must be balanced by the possible need for an image that includes a wide field of view.

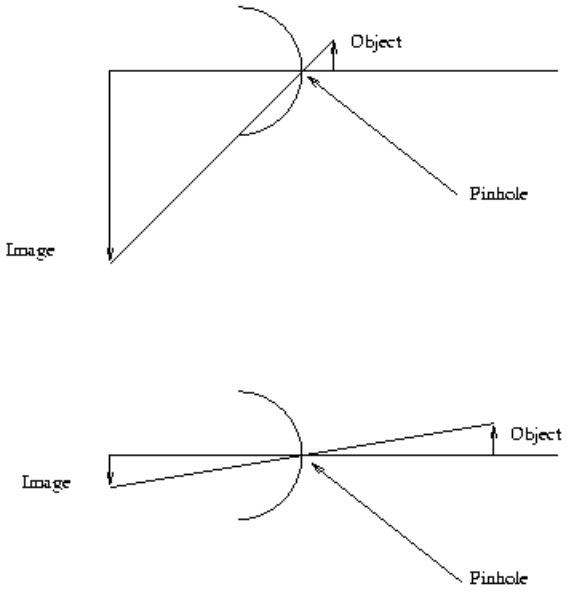

Figure 1: Different magnifications possible with a pinhole collimator depending on the location of the object with respect to the pinhole. A magnification of 6 is achieved when the object is only one unit away from the pinhole, but the magnification drops to 1 when the object is six units away from the pinhole.

Parallel hole collimators have been used to advantage with gamma-ray detectors, and their sensitivity does not depend on how closely centered the object is to the detector. Images from parallel hole collimators also do not suffer a rapid attenuation of sensitivity when the object is placed off center with respect to the collimator.

This project has several objectives. Pinhole collimators have been designed by experimenters and built by the William and Mary Physics Machine Shop. Various lucite phantoms, used to simulate a mouse tagged with radioactive markers, were designed and constructed to test the effectiveness of the pinhole collimators. A computer simulation

has been written to determine if the increased magnification that pinhole collimators offer is enough to offset the requirements of having to center the pinhole collimator with the imaged object. This requirement could prove difficult in the imaging of specific mouse organs because the pancreas, liver and gut are close to each other. It could prove problematic to distinguish between the different organs because the planar images only capture two dimensions, which would limit the information available since these specific organs overlap each other.

Mathematics of Pinhole Collimators

The geometry of pinhole collimation was described by Anger [5] about forty years ago. The resolution (R_g) and the sensitivity are given by the following equations (see Fig. 2).

$$R_g = (a + b)d_e/a \qquad (1.1)$$

in which:

R_g is the collimator resolution, a is the distance from the pinhole aperture to the front of the scintillator, b is the distance from the object to the pinhole aperture, and d_e is the effective size of the pinhole opening given by:

$$d_e = [d(d+2/\mu\tan(\alpha/2))]^{1/2} \qquad (1.2)$$

in which:

d is the pinhole opening diameter, μ is the total linear attenuation coefficient of the collimator material at the energy of the gamma-rays, and α is the taper angle of the pinhole.

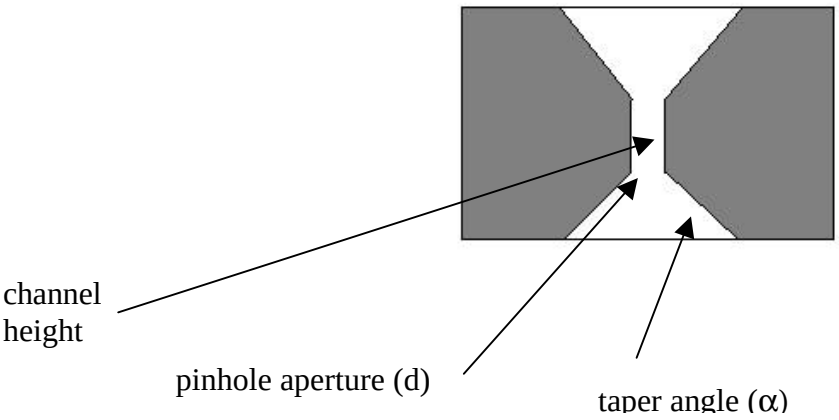

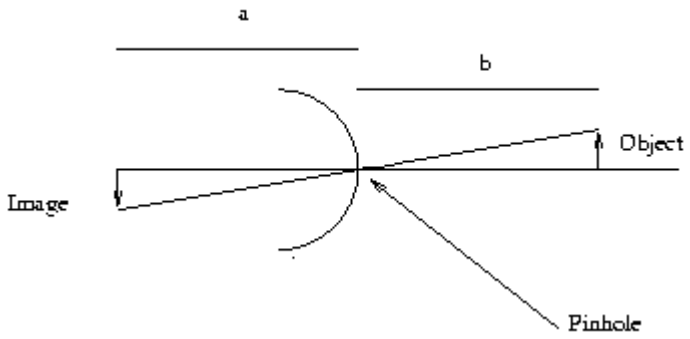

Figure 2: Diagrams of the variables listed in the equations above.

The total system resolution (R_s) is:

$$R_s = [R_g^2 + ((b/a)R_i)^2]^{1/2} \quad (1.3)$$

in which: R_i is the intrinsic resolution of the gamma camera. The camera's sensitivity depends on the distance between the aperture and the object. Geometric efficiency is the fraction of the emitted gamma-rays that is properly collimated. The on-axis geometric efficiency (g) for the pinhole collimator is:

$$g = d_e^2/16b^2 \quad (1.4)$$

The geometric efficiency had been calculated to decrease by $\sin^3(\theta)$ [6], where θ is the azimuthal angle with respect to the axis parallel with the pinhole aperture. Recent research has shown that this calculation is not completely correct. Smith and Jaszczak [7] have shown that the resolution varies by $\sin^x(\theta)$, where x is some number greater than 3. This result arises from previous underestimates of photon penetration at the edges of pinhole collimators. The variable x is not constant since it depends on the material of the collimator, the energy of the radioactive material being used, and the size of the pinhole aperture. We can predict that there should not be much deviation from the $\sin^3(\theta)$ relationship for this project, since the energy of the gamma rays are much lower than those used by Smith and Jaszczak and thus very little penetration of the brass

collimator edges occurs. Time constraints prevented the analysis of collected data that would verify this prediction.

The attenuation of photons that penetrate the pinhole collimator is related to $e^{-\mu x}$ where μ is the linear absorption coefficient of the material of the pinhole collimator per centimeter and x is the thickness of the absorber in units of centimeter. The pinhole collimators used in this project are made of brass, which is an alloy of zinc and copper. Although we do not know the exact ratio of zinc and copper, there is an upper limit of 45 percent zinc because higher amounts of zinc would make it impossible to drill the brass [8]. The linear absorption coefficient of copper at 30 keV is about 90, and zinc has an even higher coefficient because it has a higher Z. The pinhole collimators built had a thickness at the pinhole edges of between .06 to .07 cm, which would imply an attenuation factor of roughly e^{-6} or about $2.4*10^{-3}$. This factor is small enough that it can be assumed that no photons penetrated the pinhole edges.

Sources of Error

Experimental and systematic sources of error occur in this project. Sources of experimental error occur from the aparatus and the phantoms. Although precise designs were submitted for the construction of the pinhole collimators, it is impossible to construct a completely perfect pinhole collimator because the piece of brass moves as a hole is being drilled into it. These imperfections caused an uneven cut of the pinholes in the building of the collimators. Consequently, the thickness of the pinhole collimator edges depends on the location of measurement by a few percentages. The systematic sources of error come from the scattering that occurs on the edges of the pinhole collimators and from the scattering in the phantoms, which can degrade the image of the

radioactive material present in the phantoms. A reduction in the systematic error will require further experiments and computer simulations. One of our future goals is to design a computer program to filter out noise and provide more accurate images.

Computational Work

A Monte Carlo simulation has been written by me to understand the effects of varying the dimensions of the pinhole collimator and the distance separating the object and the pinhole collimator. This simulation applies only to pinhole collimators that have a non-zero channel height.

The geometry of the pinhole collimator and the distance between the imaged object and the pinhole collimator are the two main variables for determining the probability that a photon will pass through the pinhole collimator. Figure 3 shows the basic cross section of a pinhole collimator with a channel height in the xz plane.

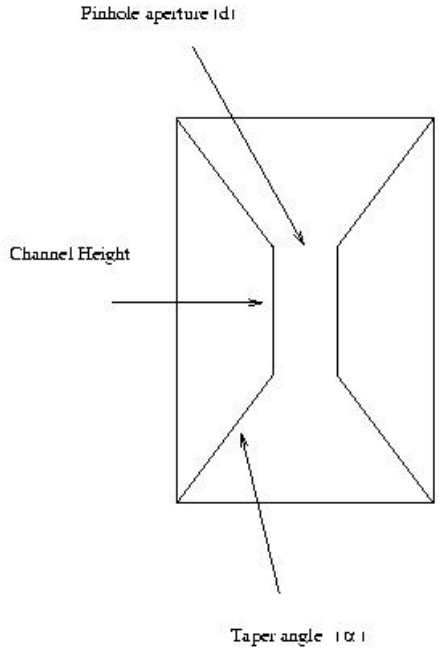

Figure 3: Cross-section of a pinhole collimator. The x-axis is pointing towards the top of the page. The y-axis is coming out of this page, and the z-axis is pointing towards the right of this page.

A larger pinhole aperture and a larger taper angle will increase the number of photons that travel through the pinhole. Pinholes with zero channel height, called knife-edge pinhole collimators, will allow more photons through. A photon that is traveling at the taper angle will pass through a knife-edge pinhole collimator, but a non-zero channel height pinhole collimator will absorb a photon that has a trajectory matching the taper angle. Since the distance between the two ends of the pinhole collimator is only about 6.35 mm for all of the collimators in this project, we can assume that it is highly unlikely that photons can bounce off the side of the pinhole collimator and have enough remaining energy to scatter on the other side of the pinhole collimator. The tangent of the two triangles in Figure 4 determines the angles that will allow the photon to pass through the pinhole collimator.

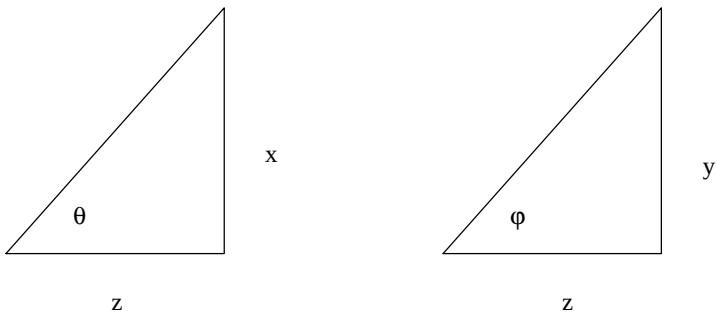

Figure 4: Two triangles representing the angles between the x and z axes and the y and z axes respectively. These are the angles from the xz and yz planes of the pinhole collimator.

Experimental Results

Test runs were taken with several different pinhole collimators. The objectives were to test the effectiveness of magnification and the limitations faced in the use of

pinhole collimators. Initially, pinholes were used on a single 25 mm tube as a first test to understand how to deal with difficulties of minimizing noise and optimizing magnification. Because the 125 mm tubes offer the opportunity to take larger images, most of the data collection focused on using the 1 mm and 2 mm pinholes on these tubes.

For the 125mm tubes, Detector B contains a parallel hole collimator, and images from Detector B are used to compare with images from Detector A. The phantoms are placed in different positions relative to Detector A in order to examine an object that is on center and off center with respect to the pinhole collimators. Different phantoms are used in order to determine the effects of scattering and the effectiveness of focusing on a specific region through the use of pinhole collimators. The raw images collected from the test runs are filtered with flood images in the KMAX data acquisition software. Flood images were taken for each detector in order to correct for the fact that the detectors do not uniformly detect photons. This discrepancy occurs because collimators and scintillators are not evenly built. An evenly distributed radioactive source is placed in the field of view of the detectors. Photon emission from the source is recorded over a period of several days, and the flood images created from this procedure indicate the necessary corrections needed to adjust for irregularities in the detectors.

These are images taken from a ten minute run on April 8, 2001 with a plastic planar phantom that has a 12 mm diameter ring depression cut into it. This ring had been loaded with about 3 μCi of ^{125}I (in late February 2001). Detector A was placed about 1 cm away from the phantom and contained a 1 mm pinhole. The pinhole was about 3 cm away from the CsI-scintillator. The ratio of the distance from the pinhole to the

scintillator over the distance from the pinhole to the object gives us an approximation of the amount of magnification by the pinhole collimator, which is 3 in this case.

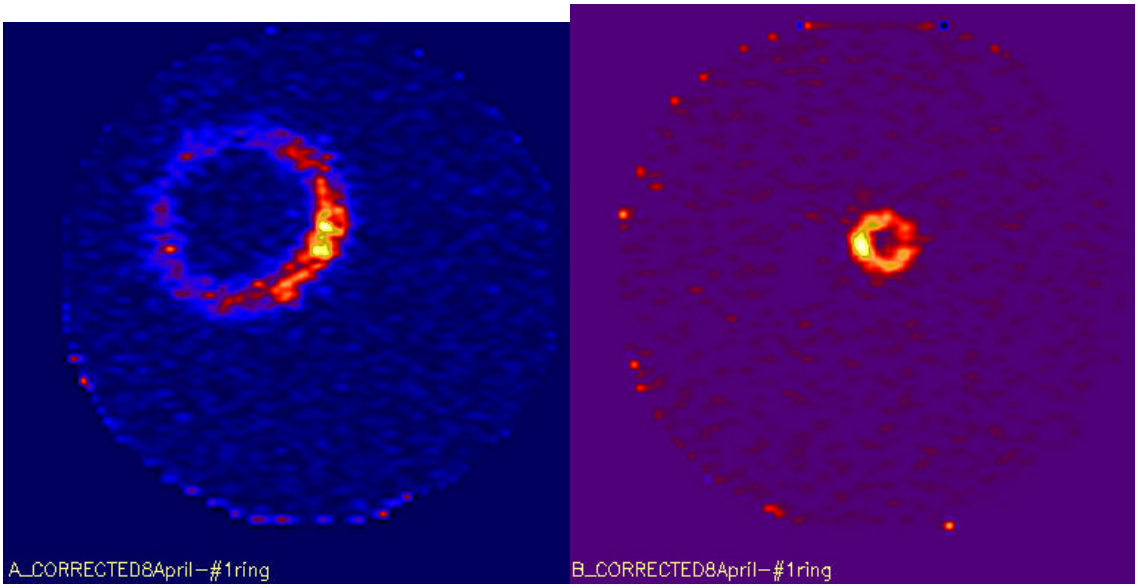

Figure 5: Images from Detectors A and B. The data were fed into a data analysis package written in IDL by Rob Saunders. The appropriate flood images were applied to filter out noise.

The orientation of the two detectors (see Fig. 5) is such that the right side of Detector A images the same area as the left side of Detector B. The actual orientation of the phantom is reflected in the image of Detector B. It appears that the ^{125}I was applied in an uneven manner because one side of the ring is hotter than the other side. Based on a rough measurement of the lengths of the rings, it appears that Detector A magnified the ring by a factor of 3 compared with the image from Detector B. The amount of counts on the left side of Detector A is significantly less than the amount of counts on the right side of detector B. The pinhole collimator has reduced the sensitivity of Detector A to particles compared with Detector B.

A 17 minute run was taken (April 3, 2001) with a phantom that contains four cavities filled with ^{125}I (see Fig. 6). Detector A is about 0.8 cm away from the top of the

phantom. This phantom is a rectangular solid with dimensions of about 2.5 mm by 2.5 mm by 10.1 mm. The four cavities are along a diagonal with each cavity shifted 0.5cm to the right and down the 2.5 cm height edge if the screws on the cavities are oriented towards the experimenter. In this orientation, the cavities would be at different distances away from Detector A. The closest cavity is 0.5 cm below the top of the phantom, which places it about 1.3 cm away from Detector A. This provides us the ability to observe how magnification changes with slight changes in the distance of separation from the pinhole collimator.

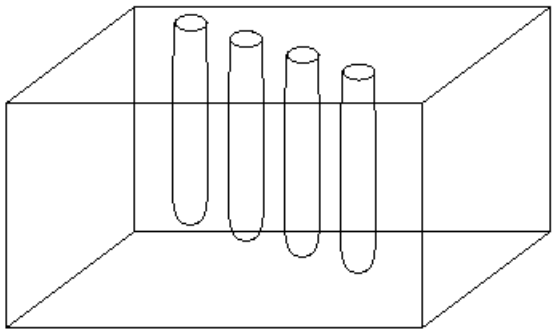

Figure 6: A rough drawing of the phantom and the four cavities that were filled with ^{125}I. Metal screws were placed on top of the cavities to seal the ^{125}I.

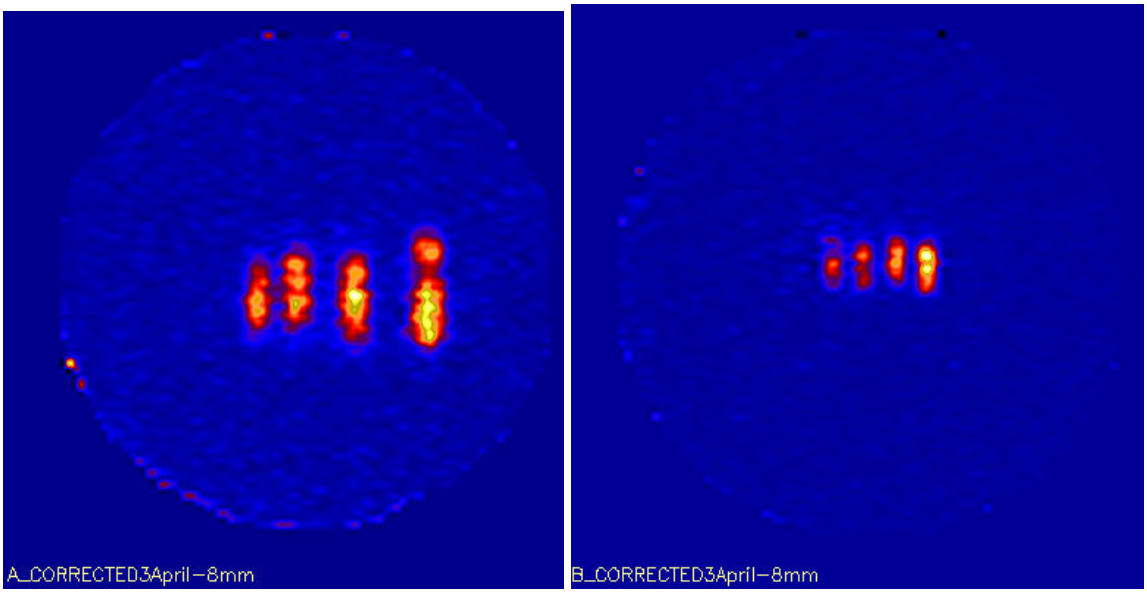

Figure 7: Images from a phantom that contains four cavities of varying distance from detector A. Although the image from detector B suggests that some of the cavities have more ^{125}I, the size of each cavity is uniform.

The results from Figure 7 indicate that Detector A is highly sensitive to small differences in distance separation from the pinhole collimator to the radioactive cavity. Since left and right are reversed for the cavities between the two detectors, the cavity furthest right in image A is actually the leftmost cavity in image B. Magnification of the largest cavity in image A is more than doubled compared with the smallest cavity in image A even though the largest cavity is only about 1.5 cm closer. Clearly, the distance between the phantom and the pinhole collimator is highly critical for getting optimal magnification.

In order to understand the difference in sensitivity between pinhole and parallel hole collimators, 10 minute runs were done to compare the imaging of the top of metal screws. The metal screws in this run were facing towards detector B, which blocks the emitted photons from reaching detector B. These images (see Fig. 8) show that detector A has successfully imaged the four cavities, but the presence of four metal screws has resulted in a noisy image in detector B as represented by the faint shaded dots present in the center of right image.

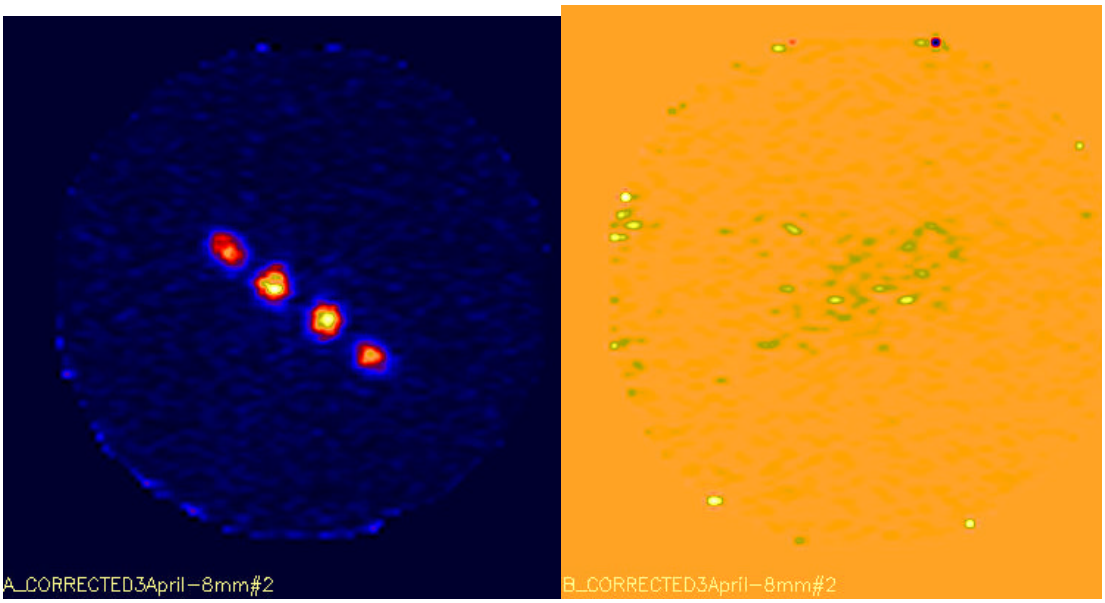

Figure 8: Image A shows the cross section of the four cavity phantom while Image B does not show any emitted photons because the metal screws block the photons from reaching Detector B.

Another run was taken with the metal screws pointing towards Detector A in order to determine if the pinhole is as sensitive to the interference from the metal screws. Figure 9 below shows that pinhole collimators are not as sensitive to shielding by the metal screws. Although the metal screws reduce the quality of the image from Detector A, the pinhole collimator picks up photons that are not directly centered over the pinhole. Parallel hole collimators only transfer the photons directly from one location on the planar grid to another. This is a distinct result with pinhole collimators, where the taper angle can allow photons to move from one side of the collimator to the other at a non-zero angle with respect to the axis parallel to the pinhole aperture.

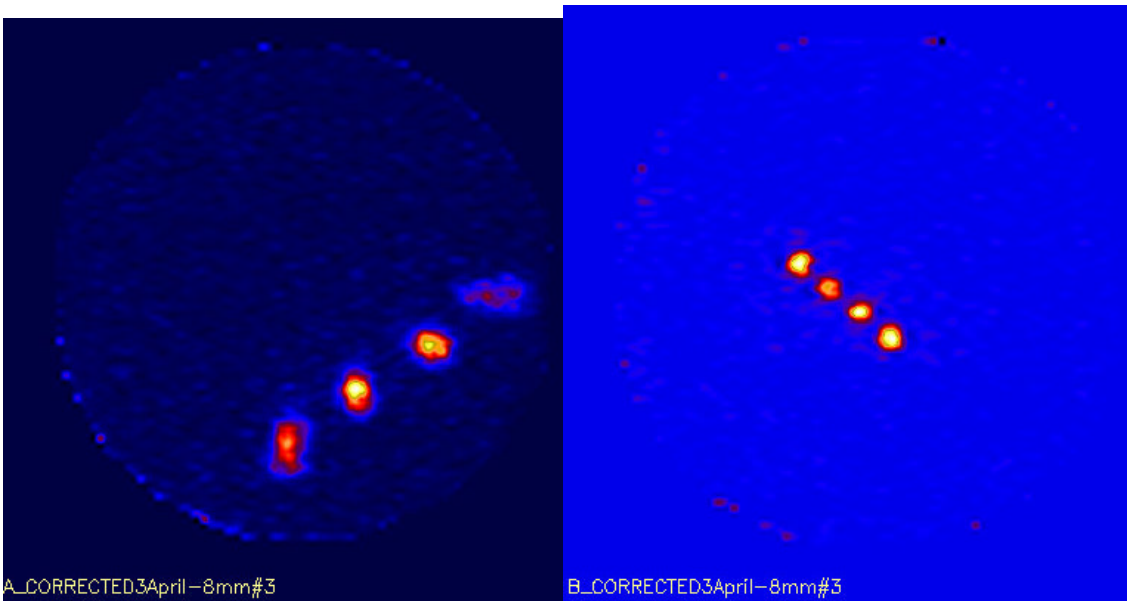

Figure 9: Results from the experiment in which the metal screws of the four tube phantom were pointed towards Detector A.

A phantom was designed with a series of dots that form the shape of a grid in order to determine the precise resolution of the pinhole collimator. The phantom is as pictured as below (see Figure 10).

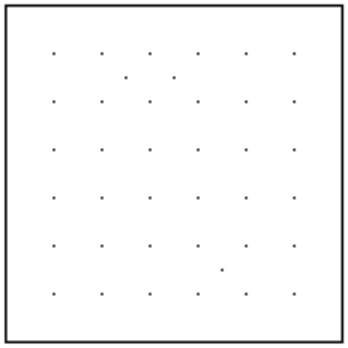

Figure 10: Schematic of phantom that has 39 1 mm diameter holes drilled into this Lucite piece. A total of 3 μCi of ^{125}I was added to all of the holes. The symmetric holes are separated by 0.5 cm from each other.

One objective was to determine the ease of imaging the three non-symmetric dots in the grid. Initially, an attempt was made to load each of the holes with equal amounts of ^{125}I. We discovered, however, that some of the holes have significantly more radioactivity

than others. Yet, this proved beneficial because it gave us the ability to distinguish different orientations of the phantom. It is possible to see that the three hottest holes from detector A are present in Detector B with the orientation reversed. The pinhole collimator magnified the image in Detector A by about 60 percent with the phantom about 2.8 cm away from Detector A (see Figure 11).

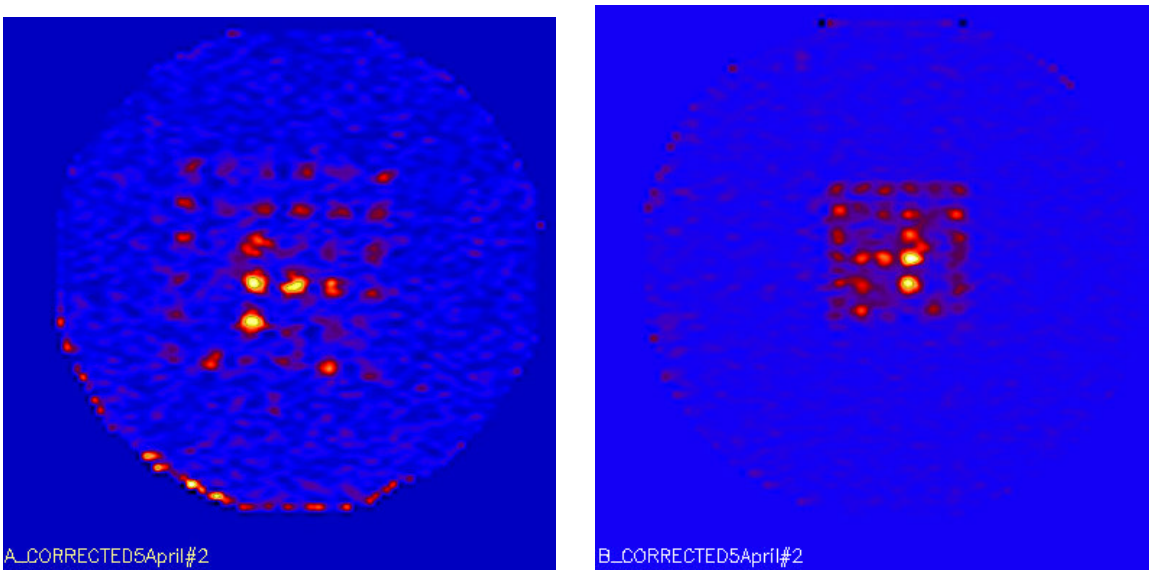

Figure 11: Images with the grid phantom at 2.8 cm away from detector A.

In another run, Detector A was placed about 0.8 cm away from the phantom. This magnified the image in Detector A by a factor of about 4 and significantly reduced the field of vision of the pinhole collimator. The three hottest dots of the phantom were captured in excellent detail in Image A because they were near the center of the pinhole collimator. The rest of the dots did not appear as well since they contain less ^{125}I and are off-center from the pinhole collimator. If the object is quite close to the pinhole collimator, the magnification and resolution of the image is exceptional when it is close to being centered with the pinhole collimator. The tradeoff occurs in the lower field of view for the pinhole collimator and the greater degradation in resolution when objects are

not centered with the pinhole collimator. This degradation also exists when there is a greater distance separating the pinhole collimator from the object, but it is not as evident in the previous image (see Fig. 12).

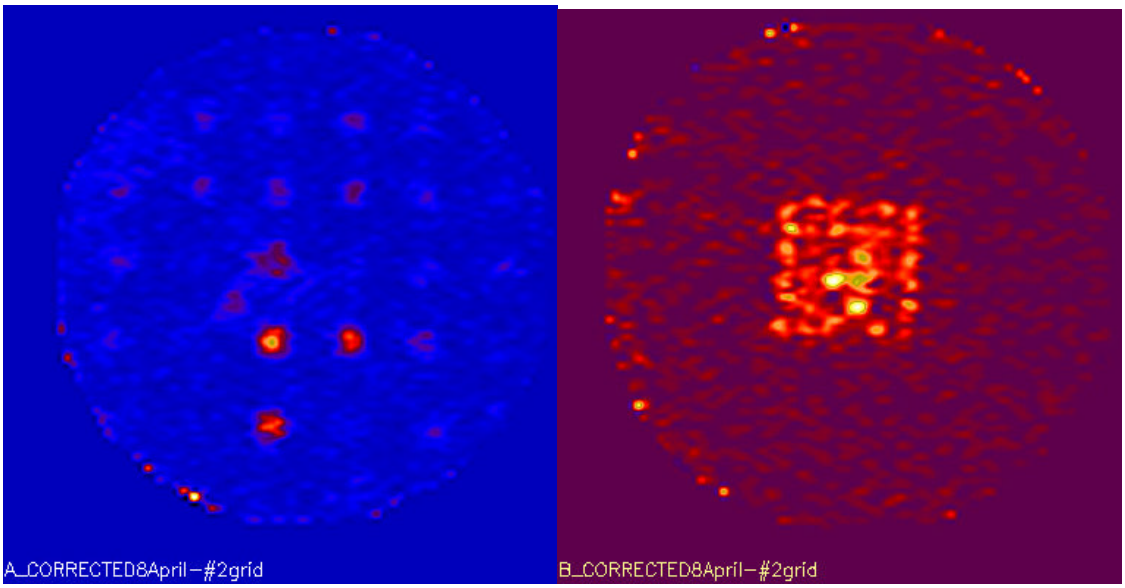

Figure 12: Images with the grid phantom 0.8 cm away from Detector A.

Discussion and Conclusions

The experimental results have verified the computer simulation showing significant attenuation in counts which reach the detector system when the imaged object is off-center with respect to the pinhole collimator. There is also a clear tradeoff between increased magnification and decreased field of view for the pinhole collimator as the object is placed closer to the pinhole collimator. Distortion occurs from scattering of photons off the object, which increases the "noise" that reach the detector. This distortion is noticeably worse when the object is placed closer to the pinhole collimator because the smaller field of view for the pinhole collimator causes the photons that arise from scattering to make up a larger proportion of the photons that pass through the pinhole collimator.

The phantoms were made from Lucite, which has a density similar to the tissue of the mice being used in biological experiments by Profs. Saha and Bradley. This similarity allows us to study possible scattering problems from the imaged material. The results from the rectangular phantom with four cavities indicates that there is little image distortion by the Lucite. This indicates that pinhole collimator imaging in a mouse would not have significant distortion by the mouse tissue.

Future Research

This project represents a first attempt at employing pinhole collimators in this project. Consequently, there is considerable potential for improving on this research. Additional phantoms can be designed to provide a better understanding of the exact nature of distortion in imaging with pinhole collimators. This information can form the basis of understanding the mathematics behind some of the systematic sources of noise. A long-term goal would be to acquire enough information from experiments and computer simulations of pinhole collimators to generate a computer program to account for the noise that results from photon scattering off the imaged object.

Single Photon Emission Computed Tomography (SPECT) is a nuclear imaging technique that rotates an object by a specific angle to take a series of planar images. The images from different angles with respect to the detector are fed into a computer program, which superimposes the images into a three dimensional picture. Robert Saunders and John Feldmann, two former participants in this research project, did preliminary work on SPECT. Much of the research on pinhole collimators have been focused on using them in conjunction with SPECT because the increased magnification would prove extremely valuable in giving clearer 3D images. Additional efforts at

reducing distortion and understanding what types of pinhole collimators are effective for different types of phantoms will give us the information necessary to the process of applying pinhole collimators to SPECT.

Appendix

The computer program listed below calculates the number of photons that pass through a pinhole collimator depending on the entered values for the size of channel height, pinhole aperture radius, pinhole collimator radius and thickness, and the distance separating the photon source from the pinhole collimator. This simulation assumes that the pinhole collimator is circular in shape.

This is the code for the computer simulation written to calculate the number of photons that would pass through the pinhole collimator.//
Pinhole Simulation.CPP

```
#include <iostream>
#include <cstdlib>
#include <ctime>
#include <math.h>
#include <stdio.h>

using namespace std;

int main()
{
        int i;
        double angle1 = 0;
        double angle2 = 0;
        float rx = 0;  //The radius of the collimator tube where 500 equals .1mm.//
        float ry = 0; //The radius in the y direction where 500 equals .1mm.//
        float rz = 0;  //This is the thickness of the pinhole aperture.//
        float px = 0;     //This is the position of the particle in the x-axis.//
        float py = 0;     //This is the position of the particle in the y-axis.//
        float pz = 0;     //This is the position of the particle in the z-axis.//
        float radius = 0;  //This is the radius of the pinhole aperture.//
        float thickness = 0;  //This is the thickness of the pinhole collimator.//
        float dz = 0;  //This is the distance separating the pinhole collimator from the
object.//
        int a1 = 0;  //This is the acceptable parameter for the photon moving in the xz
plane.//
        int a2 = 0;  //This is the acceptable parameter in the yz plane for the photon.//
        float n1 =0; //The radius of the pinhole collimator//
        int n2 = 0; //This is the maximum coordinate in the x and y axis where the photon
could be emitted.//
        int in = 0; //These variables count the number of particles that pass through the
pinhole collimator.//
        int out = 0;
```

```
        //These variables count how many particles do or do not go through the
collimator.
        float channel = 0; //This is the distance separating the two sides of the pinhole
aperture at the closest point.//
        srand( (unsigned)time( NULL ) ); //This initalizes the counter for the random
number generator.
        cout << "Please enter the distance the photon source is away from the pinhole
collimator in units of .1 mm." << endl;
        cin >> dz;  //This distance is how far away the photon is from the edge of the
pinhole
        collimator.
        cout << "Please enter the radius of the pinhole and the thickness of the pinhole"
              << " collimator in units of .1 mm." << endl;
        cin >> radius >> thickness;
        cout << “Please enter the channel height of the pinhole collimator.” << endl;
        cin >> channel;
        rx = (1000*radius)/2;
        ry = (1000*radius)/2;
        rz = (1000*(thickness+channel))/2;
        cout << "Please enter the radius of the entire pinhole collimator in millimeters."
<< endl;
        cin >> n1;
        n2 = n1*200 +1;//This variable is adjusted to turn it into an integer for the random
function.//
        angle1 = atan(rx/rz);//These two angles determine the acceptable angles for the
photons to reach the pinhole collimator.//
        angle2 = atan(ry/rz);
        pz = dz + thickness;  //This gives the total distance the photon is away from the
pinhole collimator in the z axis.//
        a1 = 20*pz*sin(angle1) + 1;  //These two variables are multiplied by 20 to scale
a1 and a2 up to the appropriate multiple
        a2 = 20*pz*sin(angle2) + 1;  //with respect to n2.//
        for( i = 0;  i < 100000;i++ )
  {
          px = (rand() % n2);
          py = (rand() % n2);
          cout << px <<"        " << py << endl;
          if ((px <= a1)  && (py <= a2))
          {
                cout <<"The particle is inside the hole." << endl;
                in = in + 1;
          }
                else
                {
                cout <<"The particle is outside the hole." << endl;
                out = out + 1;
```

```
            }
    }
        cout <<"The number of particles that went through is  " << in << endl;
        cout <<"The number of particles that were absorbed is  " << out << endl;
        return 0;
}
```

References

[1] Andrew G. Weisenberger, *Gamma-Ray Imaging Detector for Small Animal Research*, Ph.D. thesis, College of William and Mary, pg 4, 1998.

[2] Thomas F. Budinger and Henry F. VanBrocklin, *The Biomedical Engineering Handbook*, vol. 1, ed. Joseph D. Bronzino (New York: CRC Press and IEEE Press), pg 67-5.

[3] Andrew G. Weisenberger, *Gamma-Ray Imaging Detector for Small Animal Research*, Ph. D. thesis, College of William and Mary, pp 36-94, 1998.

[4] Andrew G. Weisenberger, *Gamma-Ray Imaging Detector for Small Animal Research*, Ph. D. thesis, College of William and Mary, pp 15-16, 1998.

[5] H.O. Anger, "Radioisotope Camera," *Instrumentation in Nuclear Medicine*, vol. 1, ed.
G. J. Hine (New York: Academic), pp 485-552, 1967.

[6] H.O. Anger, "Radioisotope Camera," *Instrumentation in Nuclear Medicine*, vol. 1, ed.
G. J. Hine (New York: Academic), pp 485-552, 1967.

[7] Mark F. Smith and Ronald J. Jaszczak, *The effect of gamma ray penetration on angle-dependent sensitivity for pinhole collimation in nuclear medicine*, Med Phys **24** issue 11 November 1997, pp 1701-1709, 1997.

[8] Brass, Encyclopedia Britannica (http://www.britannica.com/eb/article?eu=16479&tocid=815#815.toc), pg 2.